An Investigation into the Limitations of Tomographic Scanning for Quantitative Non-destructive Gamma-ray Measurements of High Density Radioactive Waste

S.C. Kane[1], S. Croft[1], P. McClay[1], W.F. Mueller[1], R. Venkataraman[1], M.F. Villani[1] and R.J Estep[2]
[1]*Canberra Industries Inc.*
800 Research Parkway
Meriden, CT 06450
USA

[2]*PO Box 1663 Advanced Nuclear Technology, Group N-2, MS B228*
Los Alamos National Laboratory
Los Alamos, NM 87545
USA

ABSTRACT

Accurate assay of dense heterogeneous waste forms by high-resolution gamma-ray spectroscopic techniques is made especially challenging by severe and non-homogenous attenuation of the waste material and/or a non-uniform source distribution. The development of the Tomographic Gamma Scanner (TGS) arose out of the desire to address these difficulties. By using first generation computed tomography techniques, an attenuation map of the item is constructed. This attenuation map, combined with passive emission scan data, is used to reconstruct attenuation and activity-location compensated assay values. The approach has been successfully used for non-destructive assay of low to medium density drummed waste.

In extending the method to higher densities, one faces the problem of poor counting statistics in both the transmission and emission data. The reconstructed images, which are a prerequisite to forming a representative item-specific matrix correction from the composite data, become diffuse and mottled due to poor precision and are, correspondingly, less valuable. In this work, the formation of the linear attenuation map is specifically examined using an analytical and an experimental approach. The analytical approach examined the sampling frequency of the voxel grid to understand the effects of voxel position on the attenuation map. Experimentally, a set of blocks of various materials was used to construct test patterns closely representing the mathematical model embedded in the TGS image reconstruction software. Results are presented to demonstrate the behavior of contrast resolution and spatial resolution. The dual intensity transmission technique is also discussed as a means for extending the practical density range over which the TGS can be deployed.

INTRODUCTION

In the Non-Destructive Assay (NDA) of radioactive waste, the common assumptions of both uniformity in the matrix material and distribution of radionuclides are sometimes inaccurate. Often, NDA is challenging due to severe non-uniform attenuation, for example, due to concrete or metal scrap present in the waste form. The Tomographic Gamma Scanner (TGS) can address these issues through an approach similar to computed tomography to determine the attenuation map of the waste matrix and the spatial distribution of radioactivity present. Combining this with high-resolution gamma spectroscopy, which allows identification of the discrete gamma-rays, enables energy-dependent attenuation correction and thus quantification of the gamma-emitting radionuclides present.

As the TGS technique is applied to higher densities, stronger transmission sources and/or longer count times are needed to maintain good counting statistics. Poor counting statistics in both the transmission and emission data result in poor reconstruction of the attenuation and emission maps (quantitative images) [1]. In these cases, the quantitative images become mottled and diffuse. The mottled appearance reflects non-meaningful random voxel-to-voxel scatter as the image is only defined by the available scan data in a global, or average, sense according to the algorithms to reconcile what is an over-determined problem. Radial assay bias can also emerge as the data can no longer tightly define the position of the source (e.g. to within the few voxels at the center of the item or close to the edge which is a boundary in the solution space). The result is that the activity image has a tendency to spread out into the zone of intermediate radii [2]. To address these problems at high densities, one could simply increase the intensity of the transmission beam to improve counting statistics. One way to achieve this goal in an automated general-purpose machine is known as Hybrid TGS.

In addition, two alternative approaches have been investigated to further understand the impact of high densities. These were an analytical investigation of the sampling of the voxel grid and a physical experiment to observe the spatial resolution of the TGS technique. This paper discusses each of these steps and presents preliminary results.

HYBRID TGS

The Hybrid TGS technique uses dual-intensity transmission beams with a triple-pass scan protocol to improve TGS performance at high densities. The transmission source in Hybrid TGS is of much greater activity, at least an order of magnitude, than for a typical TGS. To prevent saturating the detector for regions of the item which are less attenuating, the beam is reduced in intensity by use of a moving filter on the source store. In the triple-pass scan protocol, transmission data for each segment is collected with the low-intensity beam and then with the high-intensity beam in addition to the emission pass. The most suitable transmission data for a given view is chosen at the time of image reconstruction as selection on the fly would be too slow and incur too big a parasitic overhead given the short duration of each data grab. A full description of the Hybrid TGS technique can be found elsewhere [3].

The advantage of the Hybrid TGS technique lies in the use of a stronger transmission source, which provides better counting statistics at higher densities. Additionally the penetrability and utility of the transmission source is improved by selecting a nuclide whose emissions are concentrated in a few high-energy photons. These strategies, combined in the Hybrid TGS approach, make it possible to assay drums with fill densities beyond the historical limit of ~1g.cm^{-3}. The disadvantage is the extra time needed to perform the additional transmission pass.

As discussed in Reference 3, higher counting statistics enable better attenuation correction maps to be reconstructed from the transmission data. This can be seen in Figure 1, the attenuation maps for a 55 US gallon drum filled uniformly with sand (of density ~1.6g.cm^{-3}). The image in Figure 1a, where only low-intensity transmission data was used, displays the pronounced mottled-checkerboard effect that is not present in Figure 1b where both sets of transmission data were used for image reconstruction. These plots are ‘dithered’ to improve appearance for qualitative viewing: this involves applying a bi-cubic interpolation between the voxels which amounts to each voxel appearing as if it were composed of 3x3x3 sub-voxel.

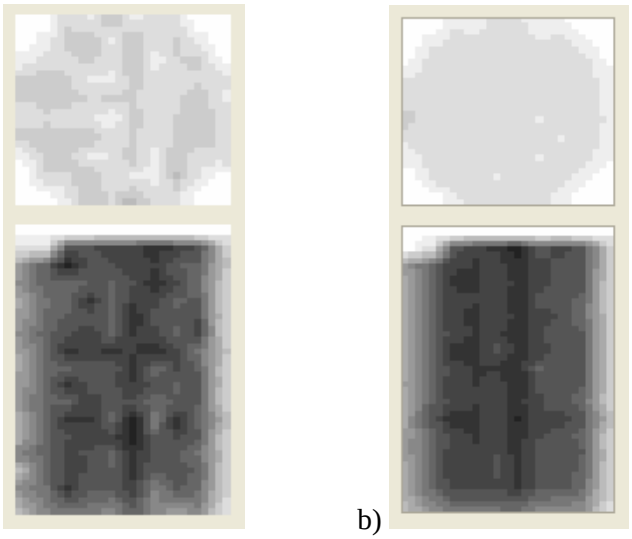

Figure 1: Attenuation Maps of a Sand (SiO_2) Filled Drum using a) Low-Intensity and b) Hybrid Transmission [3]. The upper potion of each plot is a representative cross-section while the lower part is a side projection.

ANALYTICAL INVESTIGATION OF SAMPLING

Counting statistics are only one aspect of the TGS technique that can affect assay precision. The scan pattern and resulting sampling frequency of the drum will also influence the reconstruction of emission and transmission data. Due to the design of the collimation system and scan pattern, it has generally been assumed that the sampling of the drum is essentially rotationally uniform.

To investigate whether this assumption is strictly accurate, an analysis was performed by reconstructing the "rays" between detector and transmission source at the beginning of each data grab. Figure 2 demonstrates the "ray" at the beginning of each data grab for all 150 data grabs in a single layer overlaid on the 10 by 10 voxel grid, as these are typical settings for a TGS assay of a 55 US gallon drum. The voxel grid is shown as it would be at the beginning of an assay.

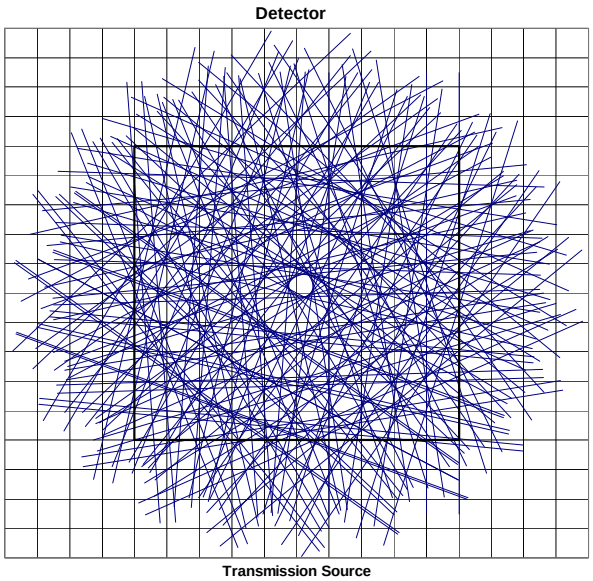

Figure 2: Representation of the Views in a Typical TGS Scan.

Figure 2 reveals the "view" pattern of the drum is, in fact, not symmetric. This is because the drum rotates in the same direction regardless of the direction of translation. To further explore this realization, the frequency with which each voxel was sampled was determined. Figure 3 shows the sampling frequency of each voxel in the form of an iso-surface plot. The lighter the area, the less frequently that voxel is sampled. The two voxels in the center of the voxel map (on the side of the detector in the Figure) are the least frequently sampled.

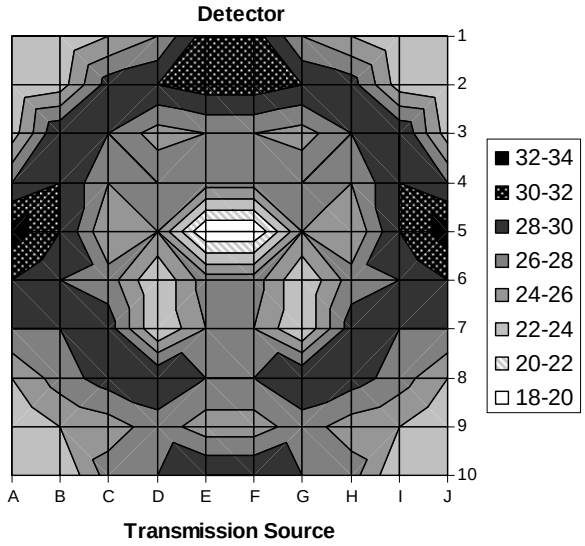

Figure 3: Sampling Frequency of Voxels. The grid is oriented as at start of an assay.

The analysis above does not take into account how much (chord length) of the voxel is sampled in a given view. The so-called thickness matrix, which is calculated by the TGS_FIT code [4], provides the sum of the path lengths traveled by a transmission photon through a given voxel during a segment scan. Figure 4 displays these values as a gray-scale iso-surface plot where the total thickness is greatest where the iso-surface is darkest.

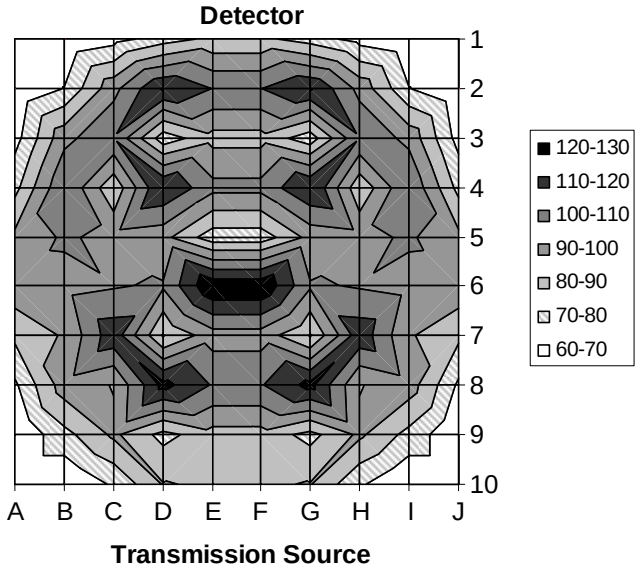

Figure 4: Iso-surface Representation of the Total Thickness (cm) Presented by a Given Voxel. The grid is oriented as at start of an assay.

Again, it can be seen that the figure is not rotationally symmetric. Not all regions of the drum are interrogated by the transmission beam equally. On the other hand, not all voxels are equally important in the *emission* image reconstruction. So this observation alone is not necessarily accuracy limiting for a given assay. It will, nonetheless, partially govern the spatial sensitivity map, which in turn feeds into the detection limit map and overall uncertainty estimate.

EXPERIMENTAL INVESTIGATION OF RESOLUTION

To explore the limits of the TGS technique further, an experiment was undertaken to examine the spatial and density resolution. The system used has been described elsewhere [2 and references therein] and made use of a 2.4 inch (60.96 mm) diamond-shaped collimator. Blocks of low-density polyethylene foam (which is virtually transparent with a density of 0.02 $g.cm^{-3}$), particle board (a reconstituted wood of density 0.6 $g.cm^{-3}$), and concrete (of density 2.3 $g.cm^{-3}$) were manufactured to approximately the same size as a typical voxel for the routine assay of a 55 US gallon drum. Enough blocks were made so that a full 10x10 voxel pattern of foam and a full voxel map of wood could be constructed on the TGS platform in such a way as to represent the mathematical model of a segment used in the image reconstruction process.

Using the representative voxel maps of foam or wood, blocks were selectively removed or replaced by a block of a different matrix, and a two-segment TGS assay was performed with the traditional (one-pass) counting time of 112.5 seconds for transmission per segment. The grid was numbered so changes to the composition of the voxel grid could be recorded. The numbering is as shown in Figure 5 where 1 through 10 represent the edge closest to the transmission source at the start of the assay and 91 through 100 represent the side closest to the detector. The grayed blocks on the edge are not used in the TGS reconstruction as these blocks lie outside of the cylindrical drum.

1	2	3	4	5	6	7	8	9	10
11	12	13	14	15	16	17	18	19	20
21	22	23	24	25	26	27	28	29	30
31	32	33	34	35	36	37	38	39	40
41	42	43	44	45	46	47	48	49	50
51	52	53	54	55	56	57	58	59	60
61	62	63	64	65	66	67	68	69	70
71	72	73	74	75	76	77	78	79	80
81	82	83	84	85	86	87	88	89	90
91	92	93	94	95	96	97	98	99	100

Figure 5: Voxel Map and Numbering Convention.

Many permutations were performed by removing a single block from a voxel map of foam, removing two blocks, replacing a single block of foam with wood or concrete, or replacing two blocks with wood. The following figures are the transmission (linear attenuation coefficient) maps of segment 1 of 2 for a few examples of these configurations. Blocks that were removed or exchanged for a different material are indicated by boxes. The maps are based on the 122 keV transmission data from a ^{152}Eu transmission source. This modest energy line might be expected to have better contrast sensitivity for the light low atomic number matrices than one of the alternative

higher energy lines. Figure 10 shows the attenuation coefficient colorbar for Figure 6 through Figure 15.

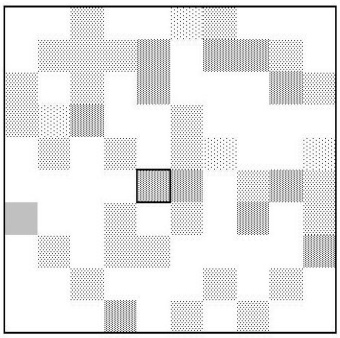

Figure 6: Foam Layer with Block Missing in Position 55.

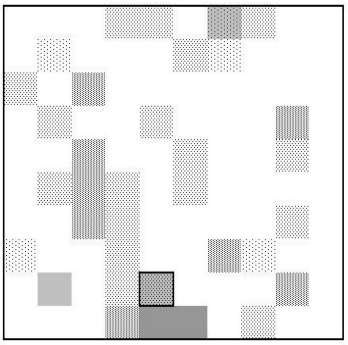

Figure 8: Foam Layer with Wood Block in Position 85.

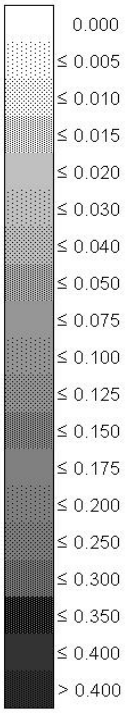

Figure 10: Attenuation Key.

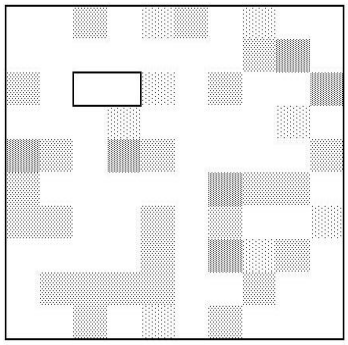

Figure 7: Foam Layer Missing Blocks in Positions 23 and 24.

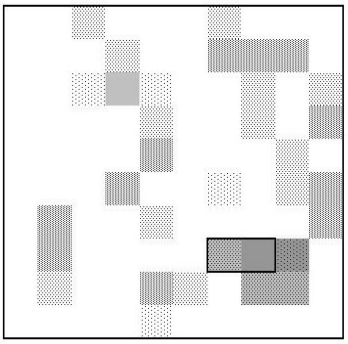

Figure 9: Foam Layer with Wood Blocks in Positions 77 and 78.

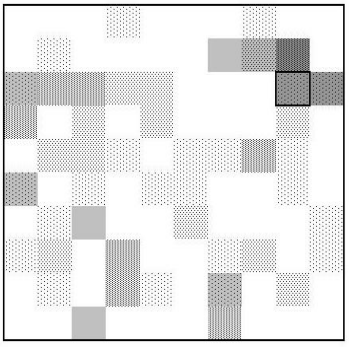

Figure 11: Foam Layer with Concrete Block in Position 29.

The same procedure was performed using the wood blocks as the base voxel map. The following figures show the 122 keV attenuation images for a few examples of these configurations. Again, blocks that were removed or exchanged for a different material are indicated by boxes.

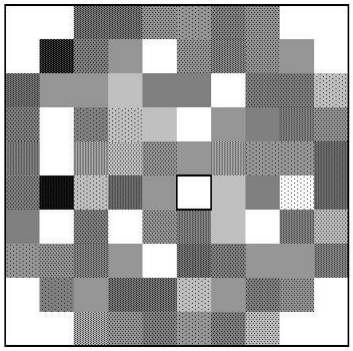

Figure 12 Wood Layer Missing Block in Position 56.

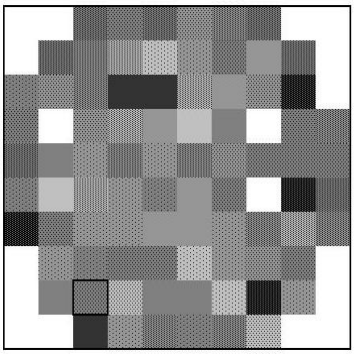

Figure 13 Wood Layer with Concrete Block in Position 83.

Lastly, to investigate how higher densities on the outside of the voxel map would affect the attenuation images, concrete blocks were placed on the outside of the wood block layer. Figure 14 shows this scenario. Figure 15 shows a similar setup except that all but the concrete blocks have been removed.

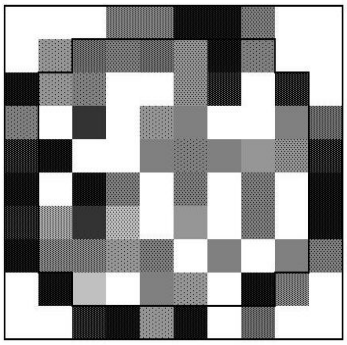

Figure 14 Concrete Blocks Surrounding Wood Layer.

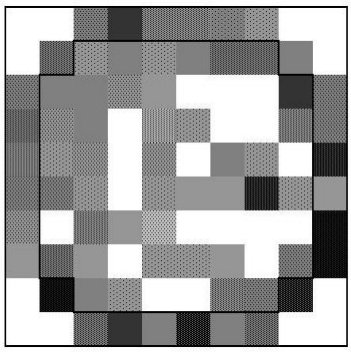

Figure 15 Concrete Blocks Surrounding Air.

The higher energy transmission images were also examined for Figures 14 and 15. The same images were present in the higher energy lines as are shown in the 122 keV transmission images, only the contrast between low and high density was poorer due to smaller attenuation coefficients for the higher energy gamma-rays.

OBSERVATIONS AND CONCLUSIONS

From these experiments, which are not confounded by activity inside the item, it appears that the attenuation correction "spreads" when a difference in attenuation is present towards the edge of a drum. This can be seen in almost all Figures presented in the previous section. The "spreading" is indicative of the radial bias reported elsewhere [2].

The transmission source used in the present experiments was a 6 mCi ^{152}Eu source, which is weaker than typically used in TGS or Hybrid TGS systems. As a result, the attenuation images for the wood block layer already begin to show the mottled-checkerboard effect. The lower counting statistics due to attenuation can be seen in Figures 12 through 15. This affect is worse in Figures 14 and 15 where concrete surrounds a lower-density matrix. The concrete acts as a type of shield, preventing adequate interrogation of the inner matrix with this transmission source.

Had a Hybrid TGS system been available for experiment, the mottled-checkerboard effect would not have been present at the densities investigated in this experiment. Due to the magnitude of the transmission source, the counting statistics would be significantly improved leading to a

higher fidelity attenuation image. A major benefit results by simply changing the transmission source from ^{152}Eu to ^{60}Co, regardless of increasing the activity of the source, as the latter emits 130% more photons in the principle high energy lines (1173 keV and 1332 keV) than the former (1112 keV and 1408 keV). The low energy lines do not transmit yet consume the straight through beam (unattenuated) counting rate dynamic range.

The experiment somewhat supports the assumption that the spatial resolution of the transmission map is just greater than the size of a voxel in the mathematical grid. Further experimental and simulation evaluation of the data is required before an overall conclusion can be drawn on the spatial and density resolution of the TGS technique for integrated transmission and emission mapping. For instance, although it has been shown that the transmission scan does not uniformly sample the layer, it is also true that not all voxels contribute equally to the modulation of a particular source distribution. The combined effects are correlated and, consequently, difficult to unravel in a generic sense, requiring further investigation.

REFERENCES

1. R. Venkataraman, M. Villani, S. Croft, P. McClay, R. McElroy, S.C. Kane, W. Mueller, and R.J. Estep, "An Integrated Tomographic Gamma Scanning System for Non-Destructive Assay of Radioactive Waste," Accepted for Publication in *Nuclear Instrumentation and Methods in Physics Research A.*
2. R. Venkataraman, S. Croft, M. Villani, and R.J. Estep, "Performance Study of the Tomographic Gamma Scanner for the Radioassay of Drums," Proceedings of 45th Annaual INMM Meeting, Orlando, FL, 18-22 July 2004.
3. S. Croft, S.C. Kane, P. McClay, R.J. Estep, W.F. Mueller, M.F. Villani, and R. Venkataraman. "Extending the Dynamic Range of the TGS Through the Use of a Dual Intensity Transmission Beam." INMM'47 Annual Meeting, Nashville, TN, July 2006.
4. R.J. Estep, "User's Manual for TGS_FIT version 2.0." LANL Report LA-UR-00-4792.